analytical chemistry

Article

pubs.acs.org/ac

Automated Quantitative Enzyme Biosensing in 24-Well Microplates

Somjai Teanphonkrang[†,‡] and Albert Schulte*[,†,‡,§]

[†]School of Chemistry, Institute of Science, [‡]Biochemistry−Electrochemistry Research Unit, Institute of Science, and [§]Center of Excellence (CoE) in Advanced Functional Materials, Institute of Science, Suranaree University of Technology, Nakhon Ratchasima 30000, Thailand

ABSTRACT: We report a novel system for glucose estimation in model and real samples, utilizing enzyme-modified pencil leads (PL) as effective electrochemical biosensors for robotic substrate quantification in 24-well microplates. Electrochemically formed carboxyl groups on the surface of the graphite were cross-linked to amino groups in the enzyme so as to attach glucose oxidase to the PL surface. Automated amperometric sensing of glucose solutions in microtiter-plate wells used computer-controlled stepper motors to move the biosensor/counter/reference electrode assemblies sequentially between the samples. This setup achieved stable analyte response and, in calibration trials, a linear response range and detection limit of 0.1−8 mM and 0.05 ± 0.01 mM, respectively. The biosensor microplate assay offered accurate "hands-off" evaluation of 4 or 20 samples per plate run, in the standard addition or calibration curve mode, respectively. Mode-independent glucose assays in standard solutions and human serum samples worked reproducibly with close to 100% recovery. The choice of cheap and practical PL enzyme biosensors and simple nonmicrofluidic measurement automation offers a convenient, labor- and cost-efficient form of quantitative biosensing, with a reduced risk of operator errors. The robotic approach is best suited to repetitive measurements of sample series, with academic research and clinical, environmental, pharmaceutical, or biotechnological analysis being potential areas for future exploitations of the methodology.

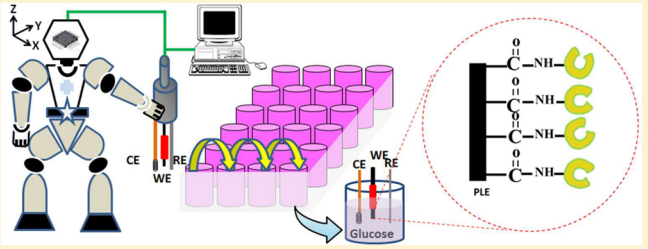

The automation of measuring procedures is a long-standing methodical challenge for analytical chemists.[1−5] The stimulus for nonmanual approaches is the need for economical, convenient, and accurate quantitative analysis of the many analytes that are assayed in environmental, pharmaceutical, and biotechnological samples in industrial and public screening units and in academic research laboratories. Computer-controlled microfluidic systems, in which all the analytical steps take place in electrochemical flow cells,[6−10] are a standard approach for automated electroanalysis. Other reported methods include the use of multiplexed electrochemical sensor microarrays paired with nonmanual flow-based delivery devices or automated pipetting stations,[11−13] microtiter plates with multiplexed three-electrode sets incorporated in the well lids,[14] or arrayed voltammetric analyzers with automated electrochemical cell operation and sample dosing.[15,16] We recently reported robotic quantitative electroanalysis of food antioxidants,[17,18] environmental heavy metals[19] and drugs,[20] using a workstation[21] in which a three-electrode assembly is moved through microplate wells by computer-controlled stepper-motors. In this system cylindrical, unmodified or bismuth and carbon nanotube-modified pencil lead (PL) electrodes served as detectors for amperometric or voltammetric analyte quantification.[17−20]

All of the electroanalysis strategies mentioned achieved useful automation levels, and the best choice for a particular analytical application will depend on the type of sample to be analyzed. Large sample numbers (>100) may be best handled with flow-based systems, whereas microplate-based voltammetric assays, which offer ease of use but have limited sample capacity, are most useful for analysis of <100 samples. The construction of microplates equipped with a set of three electrodes in each well is impractical, and problems would arise in comparing voltammetric signals arising from multiple electrodes. It is therefore worth exploring the options for automated electroanalysis, whether as advancements of current designs or as entirely novel solutions.

There are rather few examples of the controlled operation of electrochemical enzyme biosensors in microplate wells. In 2005, Castillo et al. described a planar electrode array in a 24-well microtiter plate, modified with glutamate oxidase/horseradish peroxidase in a redox hydrogel, for quantification of glutamate release from cultured nerve cells.[22] Subsequently Pemberton et al. described the use of microfabricated amperometric glucose biosensor boards attached to bottomless cell culture plates for amperometric monitoring of glucose metabolism.[23] Both systems have potential in assaying cell growth and metabolism, but their widespread application is unlikely because of the complexity of construction and the need for access to microfabrication facilities, whereas the purchase of customized biosensor microplates would be unfeasible for many laboratories. In contrast, our proposed robotic microplate-based

Received: November 26, 2016
Accepted: April 6, 2017
Published: April 6, 2017

DOI: 10.1021/acs.analchem.6b04694
Anal. Chem. 2017, 89, 5261−5269

Scheme 1. Illustration and Plan of the Developed Workstation for Robotic Amperometric Enzyme Biosensing in 24-Well Microtiter Plates and Depiction of the Procedure Used for the Construction of Glucose-Oxidase-Modified Pencil Lead Glucose Biosensors

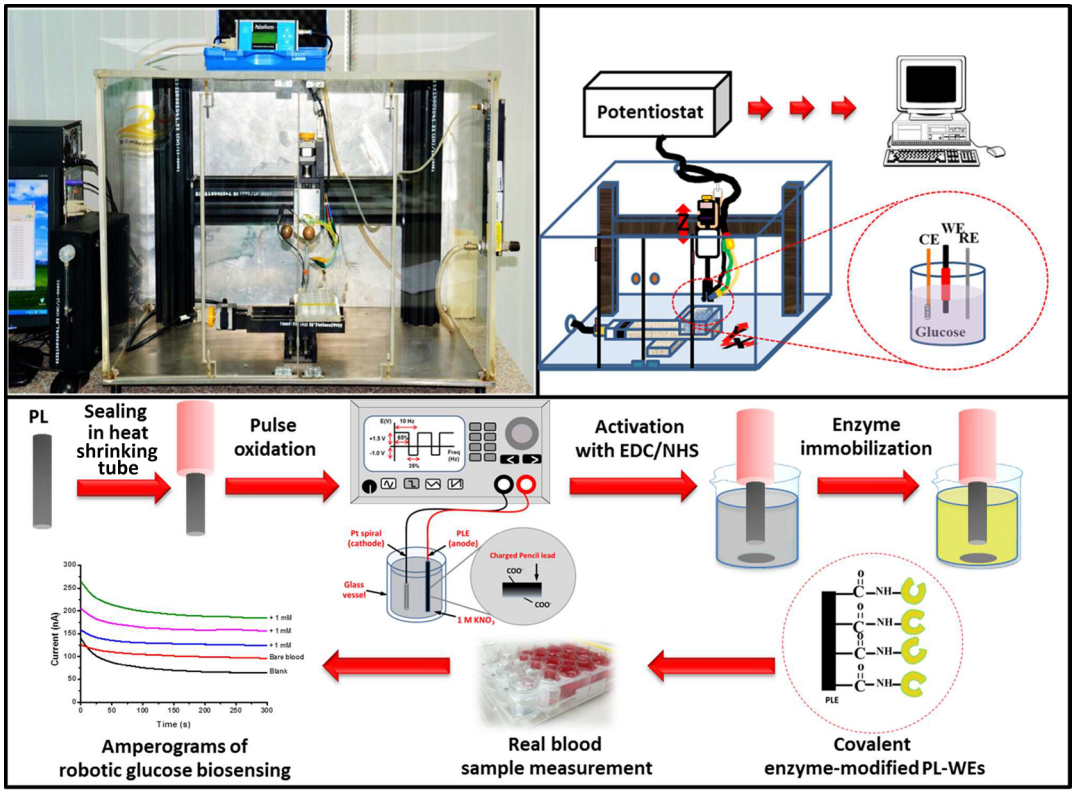

biosensor assay would, once the setup is assembled and programmed, be easy to operate and convenient for repetitive use. The machine works with standard 24-well plastic microtiter plates, without modification, and the three-electrode assembly can be quickly replaced when necessary. The biosensor transducer itself can be a micro- or macroelectrode, of optional geometry (disk or cylinder), and with an unmodifed or chemically modified surface. The adaptability and convenience of use of the proposed system make it an ideal automated tool for quantitative enzyme-based biosensing, which in some situations is regularly applied to large numbers of samples. The fabrication of suitable biosensors for the movable three-electrode assembly and the development of operational protocols for sample assessments in individual microplate wells were the crucial steps in establishing the targeted robotic biosensing scheme (Scheme 1).

Pencil lead (PL) electrodes were used because they performed very well in unmodified or modified form in robotic determinations of vitamins, heavy metals, and drugs.[17−20] PL biosensors for urinary or plasma oxalate,[24] hydrogen peroxide,[25] and glucose[26] have been reported, but all of these employ complex enzyme immobilization structures that involve, for example, delicate graphene oxide or gold nanoparticles and/or bound redox mediators as special matrix components. In the present study, a novel, simpler fabrication strategy has been employed, involving the coupling of carboxylate groups, generated on the surface of the graphite by anodic oxidation, to side-chain amino groups in glucose oxidase through carbodiimide/succinimide-directed cross-linking. This technical note describes the calibration of the novel PL glucose biosensors and reports their analytical figures of merit. Automated stability tests showed a sensor response that was stable enough for repetitive, hour-long amperometric recordings during successive microplate well runs, and robotic glucose amperometry in the standard addition, and calibration mode has been applied to both model samples (standard glucose solutions) and real samples (human blood serum), to demonstrate the general applicability of the scheme to small-scale sample sets.

2. EXPERIMENTAL SECTION

2.1. Reagents, Materials, and Solutions. Glucose oxidase (GOx; type X-S from *Aspergillus niger*, E.C. 1.1.3.4, lyophilized powder, 136.3 units/mg) and all salts for solution preparation were analytical grade products, obtained from S. M. Chemical Supplies Co. Ltd. (Bangkok, Thailand). Anhydrous analytical grade D (+) glucose was from Carlo Erba Reagenti SpA (Rodano, Italy) and bovine serum albumin (BSA) and the water-soluble cross-linkers 1-ethyl-3(3-dimetylaminopropyl) carbodiimide hydrochloride (EDC) and *N*-hydroxy-succinimide (NHS) from Acros Organics (NJ, U.S.A.). Standard heat-shrink tubes, as used in electrical engineering for wire/joint insulation, and 0.5 mm-diameter pencil leads (Pentel HB, Pentel Co. Ltd., Tokyo, Japan) were used for the fabrication of the PL-WEs that were the basis for the glucose biosensor assembly.

Stock buffer and electrolyte solutions were made up in ultrapure deionized water. Glucose stock solutions (1 M) were prepared in 0.1 M phosphate buffer solution (PBS) pH 7.4, which, supplemented with 0.1 M KCl, was also the standard medium for amperometric glucose biosensor calibration trials and sample analysis. Human blood samples were from healthy volunteers in the medical laboratory of the Suranaree

DOI: 10.1021/acs.analchem.6b04694
Anal. Chem. 2017, 89, 5261−5269

University of Technology Hospital in Nakhon Ratchasima, Thailand, and their glucose content, measured with the clinical standard procedures, was used as a reference. Blood serum, the real sample of this study, was prepared from the clinical blood samples by the standard isolation protocol.

2.2. Instrumentation. The measuring device in the robotic electrochemical workstation was a PalmSens three-electrode potentiostat (PalmSens BV, Utrecht, The Netherlands). Three computer-controlled micropositioners with stepper motors (Owis GmbH, Staufen im Breisgau, Germany) allowed up−down (z), left−right (x), and backward−forward (y) movements of a three electrode assembly over a standard disposable 24-well plastic microtiter plate with 2.5 mL vials. The working electrode was the PL glucose biosensor, the counter electrode a coiled platinum wire, and the reference electrode a AgCl-coated silver wire. The system's hardware and software (Sensolytics GmbH, Bochum, Germany) were synchronized so as to drive the electrode assembly sequentially from well to well, dipping into the well on arrival and recording either voltammograms or amperograms during timed halts. In-well amperometric glucose biosensor recordings were for 300s, with an acquisition rate of 10 current data points per second, and used a hydrogen peroxide detection potential of +0.6 V vs RE. For analysis, the raw time series data was processed with Origin and subjected to FFT filter smoothing with a point number of 50 before readout.

For manual electrochemical sensor inspections a beaker-type three-electrode electrochemical cell was used, together with the Reference 300 potentiostat from Gamry Instruments (PA, U.S.A.). A Hewlett-Packard 33220A function generator (Agilent Technologies, Inc., CA, U.S.A.) produced the voltage profiles used in electrochemical surface oxidation of PL-WEs.

2.3. Preparation of PL-Glucose Biosensors. In a first step, cylindrical PL-WEs, 0.5 mm in diameter and 2 mm in length, were fabricated by inserting 3 cm long pieces of the graphite rod into polymeric heat-shrink tubes of marginally larger diameter and shorter span. A short piece of the PL was allowed to protrude at the top, to be gripped by the alligator clip of the WE cable, while exactly 2 mm of the graphite rod was left uncovered at the bottom to provide the active sensing surface. A heat gun was used to shrink the tubing and produce a tight seal. In the next step, the electrodes were subjected to electrochemical surface oxidation in 1.0 M KNO_3, with a square wave potential (frequency,10 Hz; high level, +1.5 V; low level, −1.0 V; duty cycle, 65%) applied between the graphite sensors and a platinum wire spiral counter electrode. The time of the treatment, with repeated cycles of 65 ms-long oxidation and 35 ms-long reduction, was adjusted for maximal surface oxide generation. Oxidized PL electrodes were immersed in a 1 M solution of $AgNO_3$ in 0.1 M KNO_3 for 1 min, to exchange Ag^+ for H^+ on the carboxyl groups that had been generated. The efficiency of the ion exchange was monitored by differential pulse voltammetry in 1 M KNO_3.

After creation of these acidic groups they were used for GOx fixation by EDC/NHS-based covalent cross-linking, as adapted from a previously published procedure for carboxylated CNT electrodes.[24] Newly activated PL-WEs were submerged in 10 mL of a freshly prepared 10 mg/mL aqueous solution of EDC and 300 mg of NHS were added with slow stirring. The pH was then adjusted to 7.0, and 2 h at room temperature was allowed for derivatization to take place. The sensors were then washed with cold water and dipped into a degassed and stirred solution of 2 mg/mL GOx in 0.1 M PBS, pH 7.4. The coupling of the enzyme to the pencil leads was allowed to take place at room temperature over 2 h. Completed PL glucose biosensors were thoroughly rinsed with 0.1 M PBS, pH 7.4 containing 0.5% BSA and stored at 4 °C until use.

3. RESULTS AND DISCUSSION

Our objective was the creation of a robotic amperometric biosensor assay, using 24-well microplates and working electrodes that could be constructed simply and cheaply. Leads from mechanical pencils were chosen as the starting material for biosensor fabrication because of their good conductivity, cheapness, and availability in various diameters and hardnesses. This choice also depended on our previous experience in using PL-WEs for microplate-based automated voltammetric assays of antioxidants, antibiotics, and heavy metals[17−20] and also the reported use of enzyme-modified PL surfaces for electrochemical substrate measurements.[24−26] The glucose/GOx system was chosen for method development because both substrate and enzyme are inexpensive and because GOx is stable and has a high catalytic activity.

Graphitic carbon can acquire surface carboxyl groups when subjected to oxidative chemical or electrochemical treatments, and these functional groups can then be used in chemical cross-linking reactions.[27,28] The use of surface carboxyl-assisted bonding for chemically modified carbon electrode fabrication has been explored with carbon fibers,[29,30] glassy carbon,[31−33] carbon nanotubes,[34−36] and graphene oxide[37,38] but, to the best of our knowledge, not with PLs. The project therefore began with optimization of electrochemical surface oxide generation on PLs and the exploitation of the carboxyl groups for immobilization of GOx and in constructing glucose biosensors.

3.1. Pencil Lead Surface Oxidation and Enzyme Attachment. We first explored the effectiveness of pulsed potential oxidation in 1.0 M KNO_3 in increasing the number of surface carboxyl groups on PLs, compared to untreated surfaces, using an ion exchange/voltammetry test similar to that reported for equivalent assessments of pulse-oxidized carbon fibers. To induce H^+/Ag^+ exchange at the surface, untreated or oxidized PLs were immersed in a 1 M solution of $AgNO_3$ in 0.1 M KNO_3 and 1 min was allowed for binding of Ag^+. After briefly rinsing in water, the treated carbon was used as working electrodes for differential pulse voltammetry (DPV) measurements in 1 M KNO_3, and the current peaks for the reduction of bound Ag^+ were recorded. Only a small cathodic response was observed for the reduction of silver ions on untreated PLs, but a large, well-defined peak was reproducibly observed in the voltammograms from pulse-oxidized PLs (Figure 1).

Integration of the current traces for Ag^+ reduction and a comparison of the resultant peak charges indicated that the amount of Ag^+ and therefore of available cation-exchanging carboxylic groups was about 10-fold greater for functionalized PLs than for untreated examples. Continuous, as opposed to pulsed-potential driven, electro-oxidation of PLs, shown in Figure 1 by the green trace, also produced surface oxidation of PLs, although not as much as the procedure utilizing rapid switching between short oxidative and reductive square wave polarizations. The distinct advantage of the pulsed technique accords with the earlier findings made for similar treatments of, for instance, carbon fibers,[29,30] and this procedure was therefore chosen for the preparation of the PL precursors for biosensors with covalently attached GOx.

The covalent enzyme bonding capacities of untreated, 5 min DC-oxidized and pulse electro-oxidized PLs, as pre-evaluated

DOI: 10.1021/acs.analchem.6b04694
Anal. Chem. 2017, 89, 5261−5269

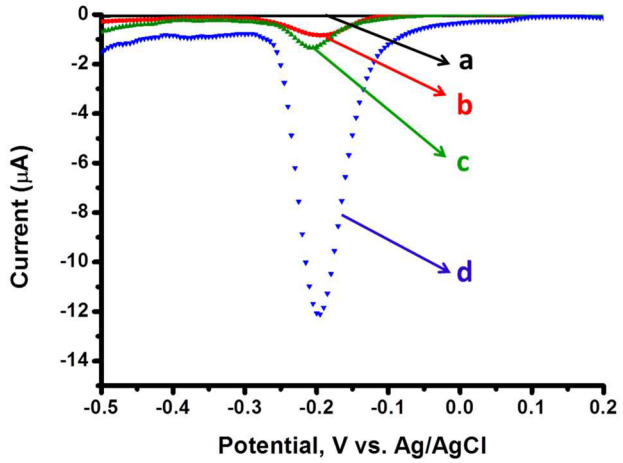

Figure 1. Differential pulse stripping voltammograms (DP-SVs) from pencil lead (PL) electrodes that had accumulated Ag^+ on surface carboxyl groups by proton-cation exchange. The voltammograms compare Ag^+ capture by unmodified PLs (red) with Ag^+ capture by PLs oxidized with 5 min DC (green) or 5 min pulsed current (blue). The black trace is from a PL that had not been exposed to Ag^+.

with the H^+/Ag^+ ion exchange voltammetry assay, were then inspected. The three different PL types were derivatized by the EDC/NHS-directed GOx immobilization reaction, and the resulting glucose biosensors were assessed in glucose calibration experiments. Figure 2 shows the amperometric responses of the GOx-modified cylindrical PL electrodes to sequential additions of small aliquots of glucose stock solution while they were immersed in continuously stirred PBS (pH 7.4) and poised at +600 mV vs Ag/AgCl pseudo reference, for the detection of enzymatically produced H_2O_2. All the biosensors responded rapidly to the incremental changes in the concentration of the substrate, glucose; the anodic H_2O_2 current increased steeply upon sugar supplementation and settled at a stable value within 5−10 s, reflecting rapid onset of the catalytic activity of GOx and efficient enzyme recycling with dissolved oxygen. From the difference in the number of available coupling groups between unmodified and differently oxidized PLs, pulse-oxidized PLs should have the largest capacity for GOx, followed by DC-treated and finally the untreated graphite rods. In agreement, the magnitude of glucose-induced H_2O_2 current steps was greatest for glucose sensors made from pulse oxidized PLs, significantly lower for DC-oxidized PLs, and very low, although still detectable, for unmodified graphite. PLs that had not been subjected to the EDC/NHS protein immobilization procedure yielded no currents steps (not shown), so that simple enzyme adsorption can be excluded as the mechanism of GOx fixation, with covalent attachment alone involved in derivatizing the modified surfaces.

Once the feasibility of PL glucose biosensor production had been confirmed, variation of the total treatment time of the pulse oxidation step was used to optimize the generation of surface carboxyl groups, so as to maximize the current signal for a given increment in glucose concentration. Figure 3 shows calibration curves for PL glucose biosensors that were fabricated from pulse-oxidized PLs with 2, 5, 15, and 30 min of electrochemical pretreatment. An increase in the saturated biosensor current occurred up to 15 min of an exposure to oxidizing potential pulses, whereas improvements in slope and width of the linear response were already optimal after 5 min of pulsed oxidation. The observed signal improvement derives from an increased number of carboxyl groups and a corresponding increase in catalytic GOx immobilization. For the chosen type and length of pencil leads, the optimal duration of pulsed oxidation was 5 min because longer treatments did not further increase the sensitivity and linearity of the PL biosensor: apparently, the upper limit of electro-oxidative generation of carboxyl groups at the carbon rod surface was reached within 5 min. This treatment time was therefore used for routine preparation of the biosensor tools for robotic amperometric glucose measurements in microplates.

3.2. Biosensor Signal Stability Tests and Calibration.

Integration of the novel PL glucose biosensors into the workstation for automated 24-well microplate electroanalysis aimed first at examining their signal stability during complete runs through loaded plates and proving the reliability of calibration curve acquisition. Figure 4A shows the microplate loading for the two initial trials. Half of the available plate wells contained 0.1 M PBS (pH 7.4) for baseline detection (A1) and electrode cleaning (A3 and 5; B2, 4, and 6; C1, 3, and 5; and D2, 4, and 6), whereas the remaining 12 slots (A2, 4, and 6; B1, 3, and 5; C2, 4, and 6; and D1, 3, and 5) contained solutions of

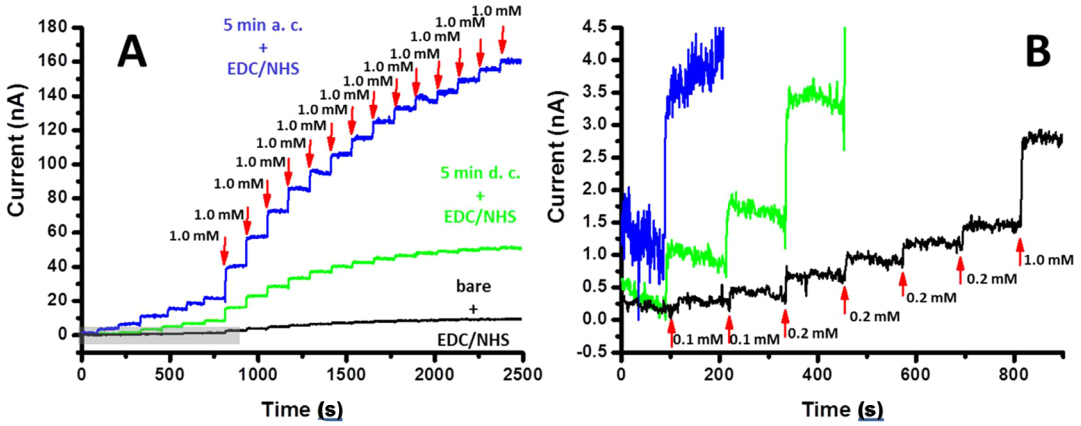

Figure 2. Chronoamperometric responses of covalently GOx-modified cylindrical pencil lead electrodes (PLs) to various concentrations of glucose. (A) Precursors for EDC/NHS-generated enzyme coupling to surface carboxyls were untreated (black), 5 min DC-oxidized (green), and 5 min pulse-oxidized (blue) PLs with accordingly different densities of carboxyl groups. (B) Zoomed-in trace of the initial few hundred seconds of the traces in (A). The working potential for H_2O_2 detection was +600 mV vs the reference electrode.

DOI: 10.1021/acs.analchem.6b04694
Anal. Chem. 2017, 89, 5261−5269

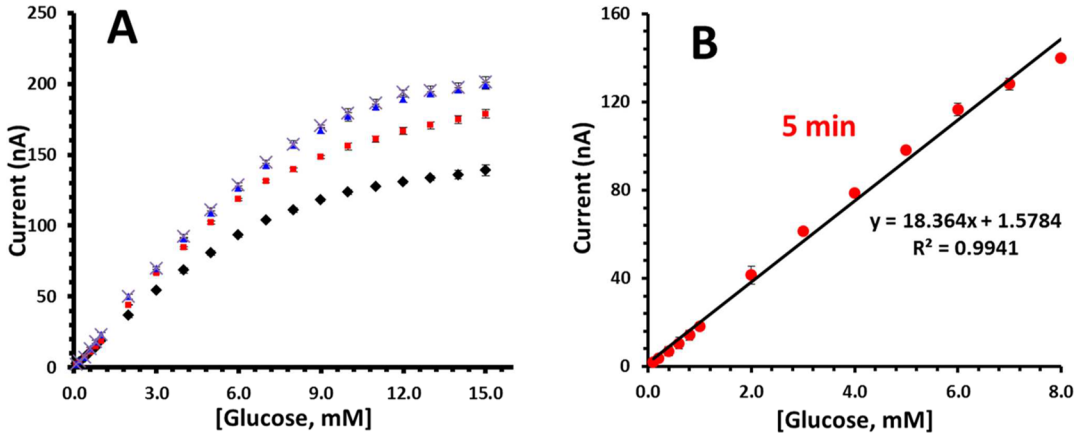

Figure 3. Calibration of PL-derived glucose biosensors (A) Background-subtracted H_2O_2 oxidation currents vs glucose concentration from covalently GOx-modified cylindrical pencil lead electrodes (PLs) after 2 (black), 5 (red), 15 (blue), and 30 (gray) minutes of pulse oxidation in 1 M KNO_3. GOx was immobilized by EDC/NHS-induced linkage to surface carboxyl groups on the graphite rods, and the H_2O_2 detection potential was +600 mV vs Ag/AgCl. Errors bars represent standard deviations of three measurements; if not clearly visible, the bars were smaller in width than the symbols used. (B) Display of the linear range of the 5 min (red) calibration plot in (A).

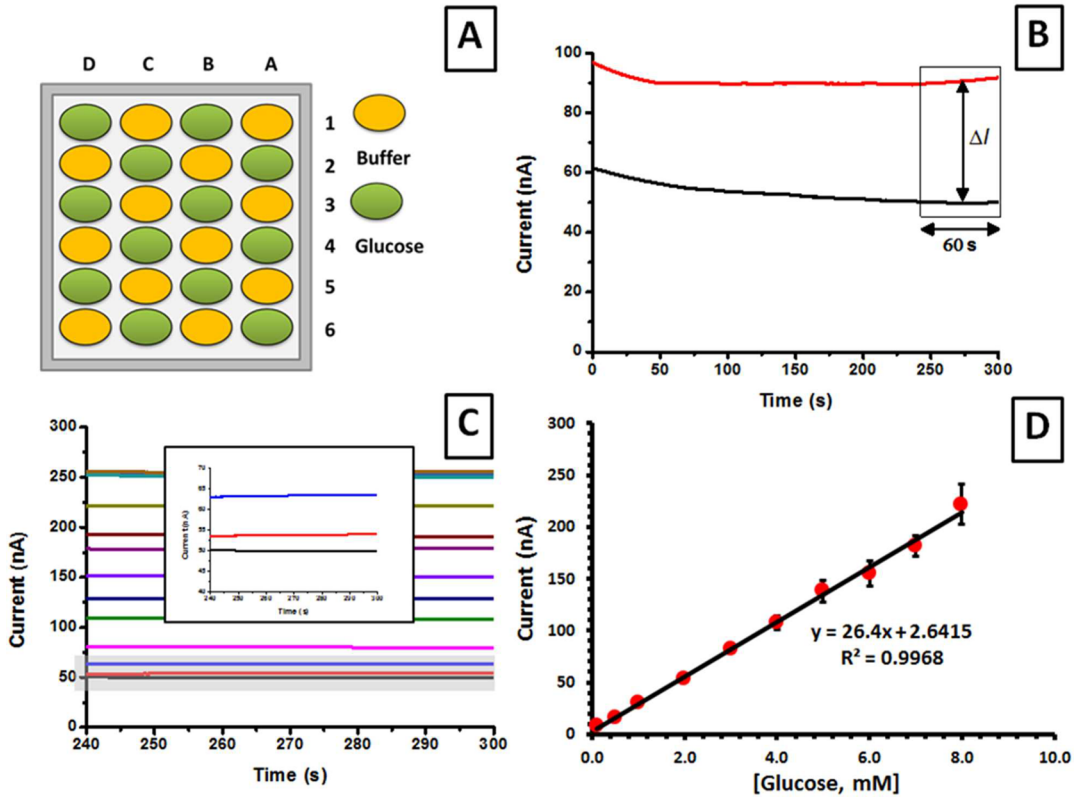

Figure 4. Automated amperometric glucose biosensing in 24-well microplates with covalently GOx-modified pencil lead electrodes. (A) The plate layout for sensor response stability testing and calibration. (B) Representative hydrogen peroxide amperograms measured during a robotic stability test plate run in wells with 0 (black) and 2 mM (red) glucose in 0.1 M PBS, pH 7.4. (C) The final parts of 12 amperograms from a robotic calibration plate run with increasing glucose concentrations. The inset is a zoom of the lower three amperograms for blank buffer (black) and buffer with 0.1 (red) and 0.5 (blue) mM glucose. (D) Plot of the means of baseline-corrected signal values from triplicate robotic glucose calibration measurements as shown in (C). The potential for the acquisition of the H_2O_2 amperograms was +600 mV vs the reference electrode.

glucose in 0.1 M PBS (pH 7.4), either all at 2 mM for stability tests or at various concentrations for calibration. The process started with manual positioning of the probe just above the surface of the solution in well A1. An adapted software script then guided the electrode set through all the wells, in the following order: A1−6, A1, B1−6, B1, C1−6, C1, and D1−6. During programmed halts in individual wells H_2O_2 amperograms (I vs t curves at constant H_2O_2 detection potential of +0.6 V vs RE) were recorded for 300 s and stored. Figure 4B shows two representative H_2O_2 amperograms from a typical robotic glucose biosensor stability test and explains their evaluation. One curve (black) was acquired in plate-well A1, containing just measuring buffer, and the other (red) from a sample well containing 2 mM glucose. Because of capacitive

DOI: 10.1021/acs.analchem.6b04694
Anal. Chem. 2017, 89, 5261−5269

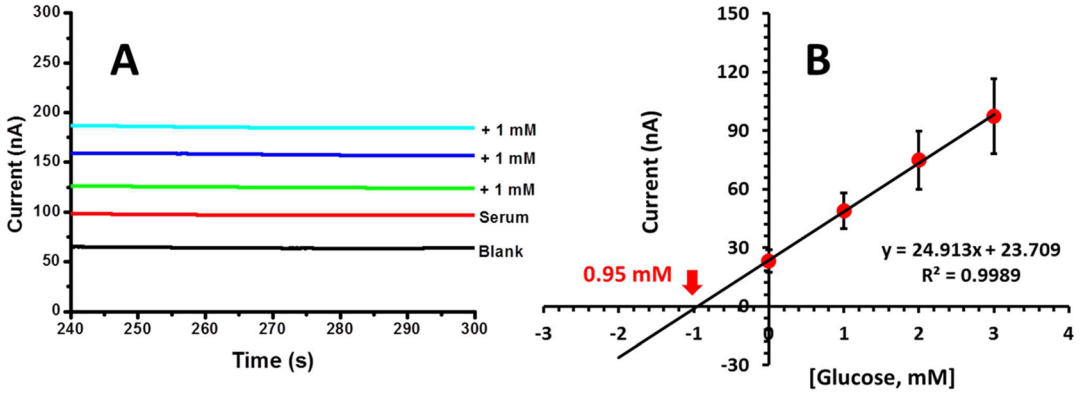

Figure 5. Robotic blood serum glucose determinations in the standard addition mode. (A) A set of amperograms with buffer alone (black), PBS-diluted blood serum (red), and the serum sample with added glucose at 1 mM (green), 2 mM (blue), and 3 mM (cyan). (B) Standard addition curve and linear regression plot for the data in (A). The measuring solution was a 0.1 M PBS, pH 7.4, and the H_2O_2 detection potential +600 mV vs reference electrode. Data points are the means and error bars the standard deviations for four nonmanual sample measurements.

Table 1. Performance of Microplate-Based Automated Glucose Biosensing in the Standard Addition or Calibration Method for the Determination of Glucose in Model and Real Samples

sample[a]	concentration adjusted	found	recovery rate (%)
standard addition method			
spiked buffer, mM (n = 12)[c]	1.00	1.05 ± 0.02	104.98 ± 8.80
serum, mM (n = 4)[d]	0.91[b]	0.95 ± 0.05	104.15 ± 5.90
spiked serum, mM (n = 4)[d]	1.00	1.89 ± 0.09	94.23 ± 9.60
calibration curve method			
blood, mM (n = 12)[c]	0.90 ± 0.01[b]	0.98 ± 0.04	108.62 ± 4.27
spiked blood, mM (n = 12)[c]	1.00	1.10 ± 0.12	103.76 ± 8.30
spiked blood, mM (n = 12)[c]	2.00	2.10 ± 0.10	103.50 ± 4.64
spiked blood, mM (n = 12)[c]	3.00	2.97 ± 0.11	98.83 ± 3.51
spiked blood, mM (n = 12)[c]	4.00	4.10 ± 0.05	102.40 ± 1.35

[a]For serum and blood values, refer to 5 times diluted samples. [b]Refers to the reference values from the provider of blood samples. [c]Four samples per microplate, triplicate plate runs, n = 12. [d]Four samples per microplate, one plate run, n = 4.

charging currents at the start of data acquisition, a gradually decaying initial current preceded the signal plateau; only the last 60 s section of the trace, lacking the nonfaradaic component, was used for analysis.

In stability tests, the analysis of 36 plateau currents, obtained by triplicate measurements with 2 mM glucose in all sample wells, gave 42.3 ± 2.1 μA as the mean value and standard deviation. The signal stability was within ±5% of the mean, suggesting there were no significant adverse effects from analyte degradation or sensor fouling during continuous operation for about 6.5 h. Automated calibration trials produced the data in Figure 4C, which shows the final 60 s of the 12 amperograms that were obtained from a microplate loaded with 0.1, 0.5, 1, 2, 3, 4, 5, 6, 7, 8, 9, and 10 mM glucose in 0.1 M PBS (pH 7.4) distributed through the wells in ascending order. Incremental changes in electrolyte glucose concentrations as small as 0.05 mM produced detectable elevations in the biosensor response but measurements with our robotic scheme were restricted to 0.1 mM as the practical lower working limit. A plot of baseline-corrected mean values of the H_2O_2 signals from triplicate microplate calibration runs against the corresponding glucose solution levels is shown in Figure 4D. Consistent with the characteristics of manual assessments, the linearity of robotically operated PL glucose biosensors extended up to 8 mM, and their sensitivity was similar, at 20.5 ± 4.2 nA mM^{-1} (n = 3). Sensor saturation at low substrate levels presumably results from the easy access of glucose molecules to the surface-anchored GOx, which is not buried within a polymeric immobilization matrix but freely accessible to dissolved species. The apparent Michaelis–Menten constant, K_m(app) of covalently GOx-modified pencil biosensors compared well with that of glucose sensors based on similarly modified graphene oxide,[39] carboxylated carbon nanotube,[40] and polymer coated glassy carbon.[41] Even if the catalytic properties of GOx are unaffected by the chemical modification of the immobilization procedure and the oxygen concentrations around the enzyme are similar, slight differences in the linear response range range and the apparent K_m for glucose may arise from dissimilarities in the density of captured enzyme molecules because of differences in the number of attachment sites on the precursor electrodes. Notably, according to a classification of the American Diabetes Association (ADA) the borderlines between normal and prediabetic and prediabetic and diabetic fasting blood glucose levels are at 5.5 mM (or 100 mg/dl) and 7 mM (or 126 mg/dl).[42] Given that serum samples are 5 or more times diluted before analysis the linear range of the PL glucose sensors of this study is suitable for the analysis of "healthy" and "diabetic" blood.

3.3. Automated Glucose Determinations in Microplates in the Standard Addition Mode. With the stability, linear range, and sensitivity of the novel methodology established, we investigated the sample recovery during robotic glucose quantification in model and real samples. Initially, 1 mM glucose in 0.1 M PBS (pH 7.4) (type 1 sample), pure

DOI: 10.1021/acs.analchem.6b04694
Anal. Chem. 2017, 89, 5261−5269

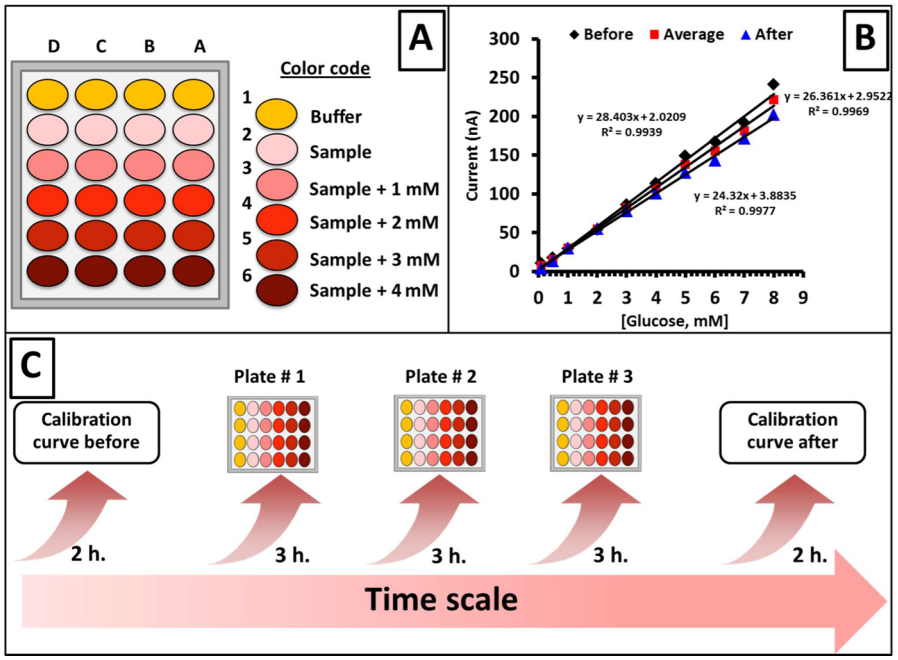

Figure 6. Setup and use of robotic, microplate-based amperometric glucose biosensor. (A) Microtiter plate loading used for glucose quantification in calibration mode. (B) Calibration plots of the peak currents as a function of glucose concentration obtained before and after blood sample measurement. (C) Sequence of operations over 13 h, during glucose biosensor quantification with calibration.

blood serum (type 2 sample), or glucose-supplemented blood serum (type 3 sample) was assayed by triplicate robotic microplate runs in the standard addition mode, with an adapted microplate layout. For electrode assembly, cleaning and baseline acquisition all wells in rows 1 and 2 contained 0.1 M PBS (pH 7.4). The wells in row 3 contained samples without glucose addition while those in rows 4 to 6 contained samples supplemented with standard glucose. One automated "standard addition" microplate run lasted 3 h and produced the data needed to construct standard addition plots for four samples. Figure 5A shows a representative set of amperograms acquired robotically during a typical "standard addition" trial on a type 2 sample. The standard addition plot for the plateau currents in Figure 5A is shown in Figure 5B. Extrapolation of the regression line to zero current indicated a glucose concentration of 4.75 mM, taking into account the previous 5-fold dilution of the sample in PBS, compared with 4.56 mM, the value stated by the hospital laboratory that supplied the blood sample. Table 1 shows a complete triplicate robotic test of the biosensors with type 1−3 samples, with acceptable recoveries of 95−105% for both model and serum samples. The novel methodology therefore has the potential for operator-free analysis of real samples.

3.4. Automated Glucose Measurements in Calibration Mode. The strategy described above was limited to the processing of only four samples per plate run, with a throughput lower than is optimal for a microplate with 24 available wells. As an alternative with higher sample throughput, we therefore explored the adaptation of the robotic procedure for use in the calibration mode, with the microplate loading and analytical steps shown in Figure 6A,C. In this configuration, the four wells in row 1 of the microplate contained only buffer, whereas all the 20 wells in rows 2−6 were used for sample solutions with unknown glucose levels. To generate calibration data for the computation of the glucose levels in particular sample wells, robotic biosensor calibration was executed before and after automated sample analysis with the routines described in the section 3.2. A typical pair of pre- and postcalibration plots is shown in Figure 6B. A good match between the two linearized data sets was observed, with a small decrease in sensitivity at the higher glucose levels, but with a linear response up to 8 mM glucose, as found in the manual tests. This confirmed the response stability of the biosensor for the 13-hour duty cycle, including the two 2-h calibrations and three 3-h sample assessments. Least-squares line fits of the averaged pre- and postcalibration data were used to convert biosensor currents from particular sample wells into the corresponding glucose concentrations.

For unsupplemented and supplemented blood from a volunteer, the calculated glucose contents from robotic quantification pre- and postcalibration are shown in Figure 7. As expected, all microplate rows in an individual plate run

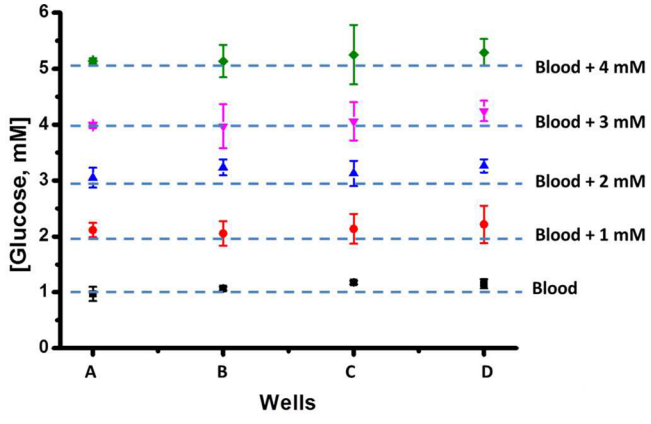

Figure 7. Robotic amperometric quantification of glucose in supplemented and unsupplemented human blood samples, diluted 5-fold. Error bars in the plot show standard deviations of three measurements.

DOI: 10.1021/acs.analchem.6b04694
Anal. Chem. 2017, 89, 5261−5269

produced concentration values that were identical within the experimental variation. The analytical performance of automated blood glucose determinations in the microtiter plate format and calibrations mode is summarized in Table 1, which provides the arithmetic means with standard deviations and calculated recovery rates for all glucose determinations. The calibration mode of automated microplate glucose biosensing provides accurate analysis of many samples with recoveries of 95−105%.

The convenience and cost-efficiency of the proposed automated amperometric biosensing is best appreciated by comparing the effort involved in manual and robotic microplate handling of the sample numbers. A triplicate microplate electroanalysis test in the calibration mode, as depicted in Figure 6C, takes about 13 h in all and delivers 100 amperograms. However, with reasonable pipetting skills and prepared sample and stock solutions, operator action is only required for about 10−15 min initially and then again after 2, 5, 8, and 11 h for microplate loading, plate exchange, and software activation, before the assay is performed with no further human intervention.

4. CONCLUSIONS

In this study, we report the construction and testing of novel amperometric glucose biosensors for automated quantitation of glucose in 24-well microplates. The glucose detectors were produced by covalent attachment of glucose oxidase to surface carboxylate groups on pulse-oxidized pencil-lead electrodes. Robotic operation of PL glucose biosensors was accomplished through their incorporation into an assembly with a Pt counter-electrode and Ag/AgCl reference electrode, sequential movement of the electrode set through microplate wells, driven by a computer-controlled stepper motor, and constant-potential amperometry when the electrode assembly was immersed in each well solution. In automated microplate runs, PL glucose biosensors displayed operational response stability over 13 h. The linear response range of the special probes was scaled to 0.1−8 mM, whereas the sensitivity and practical detection limit of the automated assay were 20−30 nA mM^{-1} and 50 μM, respectively. Depending on the choice of analytical method, the robotic glucose biosensing assay delivered reliable analytical data from either 4 (standard addition use) or 20 (calibration curve use) samples per microplate run. In either mode, quantifications in model samples and human blood serum confirmed the expected glucose values, with about 9% deviation from perfect recovery in the worst case. The automated electrochemical enzyme biosensor is a simple modular device that is reasonably cheap, easy to use, and adaptable to a wide range of analytes, through choice of the immobilized enzyme. These features make this methodology worth considering as an option in routine biosensor research and development and biosensor usages for small- to medium-scale sample analysis. The next step in improving the analytical figures of merit of robotic biosensing in microplates is the exploration of alternative biosensor designs involving functional nanomaterials.

AUTHOR INFORMATION

Corresponding Author

*E-mail: schulte@sut.ac.th.

ORCID

Albert Schulte: 0000-0002-3034-6075

Author Contributions

The manuscript was written through contributions of all authors. All authors have given approval to the final version of the manuscript.

Notes

The authors declare no competing financial interest.

ACKNOWLEDGMENTS

This work was supported by Suranaree University of Technology and by the Higher Education Research Promotion and National Research University Project of Thailand, Office of the Higher Education Commission through Postgraduate Researcher Grant to A.S. and S.T. Funding came also from allocations to A.S. from the Center of Excellence in Advanced Functional Materials. All authors express their sincere thanks to Dr. David Apps, quondam Reader, Centre for Integrative Physiology, Edinburgh Medical School: Biomedical Sciences, for his critical manuscript reading and language improvements.

REFERENCES

(1) Mellon, M. G. *Anal. Chem.* **1958**, *30*, 25A−34A.
(2) Malissa, H. *Pure Appl. Chem.* **1969**, *18*, 18−37.
(3) Stanley, R. J. *J. Autom. Chem.* **1984**, *6*, 6−13.
(4) Peris, M. *Crit. Rev. Anal. Chem.* **1996**, *26*, 219−237.
(5) Keith, L. H.; Gron, L. U.; Young, J. L. *Chem. Rev.* **2007**, *107*, 2695−2708.
(6) Del Campo, F. J. *Electrochem. Commun.* **2014**, *45*, 91−94.
(7) Trojanowicz, M.; Kołacińska, K. *Analyst* **2016**, *141*, 2085−2135.
(8) Trojanowicz, M. *Anal. Chim. Acta* **2011**, *688*, 8−35.
(9) Trojanowicz, M. *Anal. Chim. Acta* **2009**, *653*, 36−58.
(10) Chailapakul, O.; Ngamukot, P.; Yoosamran, A.; Siangproh, W.; Wangfuengkanagul, N. *Sensors* **2006**, *6*, 1383−1410.
(11) Seidel, M.; Niessner, R. *Anal. Bioanal. Chem.* **2008**, *391*, 1521−1544.
(12) Pedrero, M.; Campuzano, S.; Pingarrón, J. M. *Sensors* **2009**, *9*, 5503−5520.
(13) Danke, X.; Hongyuan, C. *Prog. Chem.* **2009**, *21*, 2379−2387.
(14) Ley, C.; Zengin Çekiç, S.; Kochius, S.; Mangold, K.-M.; Schwaneberg, U.; Schrader, J.; Holtmann, D. *Electrochim. Acta* **2013**, *89*, 98−105.
(15) Hynek, D.; Prasek, J.; Businova, P.; Zak, J.; Drbohlavova, L.; Chomoucka, J.; Kynicky, J.; Konecnal, M.; Brnicky, M.; Hubalek, J.; Vrba, R.; Kizek, R.; Adam, V. *Int. J. Electrochem Sci.* **2013**, *8*, 4441−4456.
(16) Kremplova, M.; Krejcova, L.; Hynek, D.; Barath, D.; Majzlik, p.; Horak, V.; Adam, V.; Sochor, J.; Cernei, N.; Hubalek, J.; Vrba, R.; Kizek, R. *Int. J. Electrochem Sci.* **2012**, *7*, 5893−5909.
(17) Intarakamhang, S.; Leson, C.; Schuhmann, W.; Schulte, A. *Anal. Chim. Acta* **2011**, *687*, 1−6.
(18) Intarakamhang, S.; Schulte, A. *Anal. Chem.* **2012**, *84*, 6767−6774.
(19) Intarakamhang, S.; Schuhmann, W.; Schulte, A. *J. Solid State Electrochem.* **2013**, *17*, 1535−1542.
(20) Theanponkrang, S.; Suginta, W.; Weingart, H.; Winterhalter, M.; Schulte, A. *Int. J. Nanomed.* **2015**, *10*, 859−868.
(21) Erichsen, T.; Reiter, S.; Ryabova, V.; Bonsen, E. M.; Schuhmann, W.; Maerkle, W.; Tittel, C.; Jung, G.; Speiser, B. *Rev. Sci. Instrum.* **2005**, *76*, 062204.
(22) Castillo, J.; Bloechl, A.; Dennison, S.; Schuhmann, W.; Csoeregi, E. *Biosens. Bioelectron.* **2005**, *20*, 2116−2119.
(23) Pemberton, R. M.; Cox, T.; Tuffin, R.; Sage, I.; Drago, G. A.; Biddle, N.; Griffiths, J.; Pittson, R.; Johnson, G.; Xu, J.; Jackson, S. K.; Kenna, G.; Luxton, R.; Hart, J. P. *Biosens. Bioelectron.* **2013**, *42*, 668−677.
(24) Devi, R.; Relhan, S.; Pundir, C. S. *Sens. Actuators, B* **2013**, *186*, 17−26.

DOI: 10.1021/acs.analchem.6b04694
Anal. Chem. 2017, 89, 5261−5269

(25) Teepoo, S.; Chumsaeng, P.; Nethan, P.; Prueprang, W.; Tumsae, P. *Int. J. Electrochem. Sci.* **2012**, *7*, 4645−4656.
(26) Cheng, C.; Chang, K. C.; Pijanowska, D. G. *J. Electroanal. Chem.* **2012**, *666*, 32−41.
(27) Besenhard, J. O.; Fritz, H. P. *Angew. Chem., Int. Ed. Engl.* **1983**, *22*, 950−975.
(28) McCreery, R. L. *Chem. Rev.* **2008**, *108*, 2646−2687.
(29) Jannakoudakis, P. D.; Jannakoudakis, A. D.; Theodoridou, E.; Besenhard, J. O. *J. Appl. Electrochem.* **1989**, *19*, 341−344.
(30) Jannakoudakis, P. D.; Jannakoudakis, A. D.; Theodoridou, E.; Besenhard, J. O. *J. Appl. Electrochem.* **1990**, *20*, 619−624.
(31) Narasimhan, K.; Wingard, L. B., Jr. *Anal. Chem.* **1986**, *58*, 2984−2987.
(32) Bianco, P.; Haladjian, J.; Bourdillon, C. *J. Electroanal. Chem. Interfacial Electrochem.* **1990**, *293*, 151−163.
(33) Millan, K. M.; Spurmanis, A. J.; Mikkelsen, S. R. *Electroanalysis* **1992**, *4*, 929−932.
(34) Gao, Y.; Kyratzis, I. *Bioconjugate Chem.* **2008**, *19*, 1945−1950.
(35) Lin, Y.; Lu, F.; Tu, Y.; Ren, Z. *Nano Lett.* **2004**, *4*, 191−195.
(36) Ravindran, S.; Chaudhary, S.; Colburn, B.; Ozkan, M.; Ozkan, C. S. *Nano Lett.* **2003**, *3*, 447−453.
(37) Roy, S.; Soin, N.; Bajpai, R.; Misra, D. S.; McLaughlin, J. A.; Roy, S. S. *J. Mater. Chem.* **2011**, *21*, 14725−14731.
(38) Bonanni, A.; Chua, C. K.; Pumera, M. *Chem. - Eur. J.* **2014**, *20*, 217−222.
(39) Liu, Y.; Yu, D.; Zeng, C.; Miao, Z.; Dai, L. *Langmuir* **2010**, *26*, 6158−6160.
(40) Kim, H.; Jin, J.-H.; Lee, J.-Y.; Park, E. J.; Min, N. K. *Bioconjugate Chem.* **2012**, *23*, 2078−2086.
(41) Nasri, Z.; Shams, E. *Electrochim. Acta* **2013**, *112*, 640−647.
(42) Diagnosing Diabetes and Learning about Prediabetes. Www.diabetes.org/diabetes-basics/diagnosis.

DOI: 10.1021/acs.analchem.6b04694
Anal. Chem. 2017, 89, 5261−5269